THE UNIVERSITY of EDINBURGH

Edinburgh Research Explorer

Structural capacity in fire of laminated timber elements in compartments with exposed timber surfaces

Citation for published version:
Wiesner, F, Bisby, LA, Bartlett, AI, Hidalgo, JP, Santamaria, S, Deeny, S & Hadden, RM 2019, 'Structural capacity in fire of laminated timber elements in compartments with exposed timber surfaces' Engineering Structures, vol. 179, pp. 284-295. DOI: 10.1016/j.engstruct.2018.10.084

Digital Object Identifier (DOI):
10.1016/j.engstruct.2018.10.084

Link:
Link to publication record in Edinburgh Research Explorer

Document Version:
Publisher's PDF, also known as Version of record

Published In:
Engineering Structures

General rights
Copyright for the publications made accessible via the Edinburgh Research Explorer is retained by the author(s) and / or other copyright owners and it is a condition of accessing these publications that users recognise and abide by the legal requirements associated with these rights.

Take down policy
The University of Edinburgh has made every reasonable effort to ensure that Edinburgh Research Explorer content complies with UK legislation. If you believe that the public display of this file breaches copyright please contact openaccess@ed.ac.uk providing details, and we will remove access to the work immediately and investigate your claim.

OPEN ACCESS

Download date: 05. Apr. 2019

Engineering Structures 179 (2019) 284–295

Contents lists available at ScienceDirect

Engineering Structures

journal homepage: www.elsevier.com/locate/engstruct

Structural capacity in fire of laminated timber elements in compartments with exposed timber surfaces

Felix Wiesner[a,*], Luke A. Bisby[a], Alastair I. Bartlett[a], Juan P. Hidalgo[a,b], Simón Santamaria[a], Susan Deeny[c], Rory M. Hadden[a]

[a] School of Engineering, The University of Edinburgh, The King's Buildings, Mayfield Road, Edinburgh EH9 3FG, Scotland, United Kingdom
[b] School of Civil Engineering, The University of Queensland, Advanced Engineering Building Bldg. 49, Rm. 630, St. Lucia, QLD 4072, Australia
[c] Arup, 13 Fitzroy Street, London, UK

ARTICLE INFO

Keywords:
Cross-laminated timber
Structural fire engineering
Compartment fires
Performance-based design
Heated depth
Thermal effects
Fire resistance

ABSTRACT

In compartment fires with boundaries consisting of exposed mass timber surfaces – for example in compartments with exposed cross-laminated timber (CLT) walls or floors – the thermal penetration depth, i.e. the depth of timber heated to temperatures significantly above ambient behind the char-timber interface, during fire exposure may have a significant influence on the load bearing capacity of structural mass timber buildings, particularly in the decay phase of a real fire. This paper presents in-depth timber temperature measurements obtained during a series of full-scale fire experiments in compartments with partially exposed CLT boundaries, including decay phases. During experiments in which the timber surfaces achieved auto-extinction after consumption of the compartment fuel load, the thermal penetration depth continued to increase for more than one hour, whilst the progression of the in-depth charring front effectively halted at extinction. A simple calculation model is presented to demonstrate that this ongoing progression of thermal penetration continues to reduce the structural load bearing capacity of the CLT elements, thereby increasing the potential for structural collapse during the decay phase of the fire. This issue is considered to be most important for timber compression elements. Currently utilised structural fire design methods for mass timber generally assume a fixed 'zero strength layer' depth to account for thermally affected timber behind the char line; however they make no explicit attempt to account for these decay-phase effects.

1. Introduction

Glued laminated timber (glulam) and cross-laminated timber (CLT) are increasingly proposed as primary structural framing materials for both residential and commercial buildings. This increase in the use of laminated timber is driven by a combination of site, construction, environmental, and aesthetic considerations. However, fire safety is widely perceived to limit applications of tall timber buildings, due to both the inherent combustibility of timber, as compared with non-combustible structural framing materials such as reinforced concrete or steel (both of which present their own particular challenges in structural fire engineering design), and to the historical reality that serious conflagrations have occurred in the past in cities that were constructed largely from timber (e.g. Great Fires of London, Chicago [1,2]).

The issue of structural fire safety design in tall timber buildings with significant amounts of exposed mass timber has recently been the topic of research and debate within the fire safety community. Some authors (e.g. [3]) have suggested that, rather than simply being required to demonstrate an ability to meet the prescriptive fire resistance ratings currently suggested in building design guidance, tall mass timber structures ought to be designed instead so that auto-extinction of exposed timber occurs once the moveable fuel load has burned out in a fire. The design objectives should in this case not be measured via prescriptive fire resistance requirements but rather aimed at achieving an acceptable level of safety by considering design fires more appropriate for exposed mass timber construction.

Proof of concept of the ability to achieve burn out in timber compartments with various specific configurations, and with partial encapsulation of timber surfaces by non-combustible cladding, has been demonstrated in multiple large-scale [4–6] and medium-scale [7] experiments. The available data suggest that this can be achieved at critical mass loss rates between 3.5 g/m^{2}s [6,8] and 3.9 g/m^{2}s [9] to obtain auto-extinction for fire-exposed timber (Radiata Pine in this case). The configuration of a compartment, the moveable fuel load, the

* Corresponding author.
E-mail address: f.wiesner@ed.ac.uk (F. Wiesner).

https://doi.org/10.1016/j.engstruct.2018.10.084
Received 20 March 2018; Received in revised form 27 October 2018; Accepted 30 October 2018
0141-0296/ © 2018 The Authors. Published by Elsevier Ltd. This is an open access article under the CC BY license (http://creativecommons.org/licenses/BY/4.0/).

compartment size and ventilation, the number, size, and orientation of exposed timber surfaces, and – importantly – the potential for fall-off of charred timber lamella during a fire, are all considered likely to play roles in influencing whether auto-extinction will occur for a given compartment.

A key requirement for structural design for fire in England and Wales, and most other jurisdictions globally, is that buildings should maintain stability and prevent the spread of fire for a *reasonable* period [10]. Interestingly, the corresponding European directive [11] refers to maintenance of stability for a *specific* period of time. This is to allow for safe evacuation, to protect the safety of first responders, and – although rarely explicitly stated – can be expected to provide some measure of property, environmental, and business continuity protection.

Compliance with the above requirements is typically achieved through a framework of 'fire resistance ratings' which is historically based on standard furnace testing. This is a design and assessment approach wherein isolated building elements are exposed to a specified time-temperature curve in a standardised fire testing furnace until they fail either by loss of load bearing capacity or by losing their ability to adequately maintain fire compartmentation. The temperature in the furnace can either be controlled using thermocouples [13], in which case a measure of the gas phase temperature is used as the control, or through plate thermometers [14] which provide control via the so-called adiabatic surface temperature; this represents a combination of radiation and convection temperatures. Regardless of the control instrumentation used, the achieved fire resistance rating (quoted as a duration in time) provides a relative performance assessment of the building element when tested under standardised heating conditions and in isolation. This cannot generally be directly translated into the structural performance of real buildings in real fires [15,16] for a wide range of reasons which need not be discussed here.

Structural fire design guidance documents, for example EN 1995-1-2 [17] for structural timber, currently offer both simplified and more advanced calculation methods to assess the fire resistance or variation in load bearing capacity of timber elements in fire. Guidance for both the simplified methods, e.g. the reduced cross-section method (RCSM), and the more advanced methods, e.g. non-linear finite element analysis, is strictly applicable only to standard fire exposures. Available design methods therefore represent simplified attempts to design to achieve the fire resistances that would be obtained for elements when assessed in standard furnace tests. These are thus *relative* assessments between fire resistance periods that cannot be used for design optimisation (e.g. CLT layup and compartment geometry), nor can they properly assess the structural performance of timber elements in real (i.e. non-standard heating) fires.

Furthermore, it is notable that in real fires the fire dynamics may also depend considerably on the materials of construction. Thus, standard fires may have limited relevance or applicability for mass timber buildings with exposed timber surfaces. This paper seeks to highlight various reasons why more fundamental design approaches may be needed to assure adequate structural response to fire in these situations.

2. Structural fire design for timber compression elements

When exposed to fire, timber will pyrolyse and under sufficient heating will turn to char which is typically assumed to have negligible strength or stiffness [18,19]. Beneath the char layer however, the heat-affected timber within the element will retain some fraction of its ambient temperature strength, depending on its temperature, moisture content, and the specific type and direction of loading (with respect to the grain direction in particular) [20]. The thermal (i.e. insulating) properties of the char layer, as well as the increased distance between the heated surface and the in-depth pyrolysis front, provides thermal protection to the timber beneath the char, particularly under rapid heating conditions, and results in a steep in-depth temperature gradient in the uncharred timber and a shallow *thermal penetration depth* (this may be defined as timber that is heated above ambient temperature). Available research [21] suggests that the thermal penetration depth is typically 25 to 35 mm at any time between 30 and 90 min during standard fire exposure.

The most widely used method for structural fire design of mass timber elements is the RCSM. This is currently set out in EN 1995-1-2 [17] and assumes that an effective reduction in the size of the cross section during fire can be approximated by using a constant rate of charring and 'lumping' losses in strength and stiffness of the heat affected timber beneath the char line into a 'zero strength layer (ZSL)'. Current guidance assigns a depth of 7 mm to the ZSL. The resulting reduced cross-section is then assumed to respond as though it is at ambient temperature, and its load bearing capacity is assessed using ambient temperature design methods and mechanics. The ZSL value of 7 mm was determined during the 1980s via modelling, and was 'validated' against a single test on a glulam beam in bending under standard fire conditions [22]. Several researchers have since shown that a constant value of 7 mm should not be used for timber subjected to non-standard loading or heating conditions, or particularly for CLT [23–27] in compression or hogging. As a consequence, multiple values for the ZSL have been proposed in recent years as alternatives to the 7 mm which is currently suggested for use in design. These proposals attempt to account for the loading condition [24] and the potential fire resistance (via the total thickness) [28]. In some jurisdictions, an alternative RCSM is recommended. In North America, for instance, the ZSL is assumed to vary as a function of the charring depth, and hence as a function of the required fire resistance [29,30].

3. The potential importance of the decay phase

If fire strategy designers employ a defend-in-place approach (where fires are expected to be contained within the compartment of fire origin) [3] for a mass timber building with exposed timber surfaces, then it is essential that burn out (i.e. auto-extinguishment) should occur without loss of stability or fire compartmentation. During burn out, as all moveable fuel load is consumed, the gas phase compartment temperatures will reduce and any charring of exposed timber stops (notwithstanding the potential for smouldering combustion under certain conditions that are not treated in the current paper). The heated timber below the char layer will also eventually cool, although a thermal wave will continue to transfer heat deeper into the cross section even after temperatures begin to reduce at the heated surface. This will continue to reduce the strength and stiffness of the timber element for some time beyond burnout.

The above concern has previously been noted by several researchers [31–34], however it is not yet explicitly accounted for in any widely applied timber structural fire design guidance. Results from recent furnace tests on large glulam timber columns, undertaken to simulate burnout and assess structural fire response under auto-extinction scenarios, show that in-depth temperatures continue to increase long after the fire exposure is halted [35]; in this specific case in-depth heating continues for at least 240 min after 90 min of standard fire exposure.

This thermal wave of continued in-depth heating after extinction, which has also been observed to occur for reinforced concrete [36] and protected structural steelwork [37], constitutes a hazard for timber structures. This hazard exists because significant heat induced deterioration of mechanical properties for timber can be expected at lower temperatures (i.e. from approximately 60 °C) than for structural steel or reinforced concrete (above 250 °C or higher) and the structural consequences for timber may therefore be greater where heating of deep timber sections occurs both during *and* after the burning phase of a compartment fire.

In light of the thermo-mechanical interactions highlighted above, this paper describes and then quantifies in illustrative terms the thermal wave – which can also be considered a redistribution of heat – in real burnout scenario experiments on timber compartments with significant

amounts of exposed timber. The purpose of this work is to quantify potential ongoing reductions in load bearing capacity during cooling in the decay phase. In addition, the temperature development in the cross-section and the implications of this on the load bearing capacity during the decay phase are quantified and discussed.

4. Compartment fire experiments with exposed timber surfaces

Five full-scale compartment fire experiments on CLT compartments with differing amounts of exposed CLT surfaces were performed primarily to investigate the influence of exposed timber surfaces on compartment fire dynamics and the potential for auto-extinction. Full details of these experiments are given by Hadden et al. [4].

In these experiments the CLT compartment walls were instrumented with Inconel sheathed K-type thermocouples with an outer diameter of 1.5 mm. These were inserted at specified depths via drilling from the back (i.e. unexposed) face of the timber. For this purpose 2 mm wide holes were drilled to within 8 mm of the target depth and the remaining depth was drilled to a 1.5 mm diameter. This ensured that the thermocouple could be inserted into the hole, but achieved a snug fit near the thermocouple tip. Mobile drill stands were used to ensure that the deviation angle of attack of the holes was minimised and that the drill depth was as accurate as possible. Thin skin calorimeters (TSCs) [38] were positioned on the exposed surfaces of the CLT within the compartment to estimate the incident heat fluxes to the timber during the experiments. The total heat release rate (HRR) was measured by oxygen consumption calorimetry, as was the mass loss rate for the compartment fuel load which consisted of timber cribs, flow velocities within the compartment opening, temperatures throughout the compartment in the gas-phase, and heat fluxes at specified distances outside the compartment opening. The current paper focuses on the in-depth temperature measurements in the exposed CLT walls during heating *and* cooling.

All of the CLT panels in the experiments were composed of five timber lamellae, each 20 mm in thickness and face (but not edge) bonded with a one-component polyurethane (PUR) adhesive. The timber was graded to a C24 strength class [39], and as such the lamellae can be expected to have a mean density of 420 kg/m^3. All wall and ceiling parts were stored outside for several weeks before being left indoors for several days before the experiments. The spatial mean moisture content of the CLT walls immediately before the experiments were performed was measured as 13.3% with a sample standard error of 0.3%. Ventilation was provided via a single compartment opening, 1.84 m in height (starting at floor level) and 0.8 m wide. The internal dimensions of the compartment were 2.72 m in both width and length, and 2.77 m in height. The use of slightly different encapsulation systems on protected walls between different experiments meant that these dimensions varied slightly (± 100 mm).

Each of the experiments was assigned a name according to its specific configuration in terms of the number and position of exposed internal timber surfaces. *Alpha*-configuration refers to experiments where one side wall and the back wall (i.e. opposite from the compartment opening) were exposed; *Beta*-configuration refers to the ceiling and the back wall being exposed; and *Gamma*-configuration refers to the back wall, one side wall, and the ceiling being exposed. The positions of the thermocouples across the surface of the CLT elements are shown in Fig. 1. Thermocouples for 'high density' instrumentation points (referring to the legend in Fig. 1) were placed at target depths of 5, 10, 15, 20, 25, 30, 35, 40, 50, 60, and 80 mm from the fire-exposed surface. For the 'low-density' instrumentation points the chosen depths were every 20 mm from the exposed surface. Any deviations from the targeted (i.e. desired) thermocouple depths were recorded, and the actual installed depths were subsequently used in analyses. The resulting mean vertical placement error between targeted and achieved depth was −0.4 mm with a standard error of the mean of 0.19 mm. All thermocouples were spaced at least 10 mm from each other, in order to minimise the influence on temperature readings between the thermocouples.

5. Experimental results

Of the three configurations of compartment examined in these experiments (i.e. Alpha, Beta, and Gamma), two were of these were performed in duplicate. Three distinct burning scenarios that were observed are of primary interest in the current paper; these are shown in Fig. 2. The full experimental results are given by Hadden et al. [4].

For Experiment Beta 1 with back wall and ceiling exposed, auto-extinction of the exposed timber was achieved shortly after the compartment fuel load was consumed. This behaviour is clearly evidenced by the HRR curve (Fig. 2a).

For Experiment Beta 2, which was a repeat of Experiment Beta 1, a comparable reduction in HRR was observed after the initial steady burning phase, however char fall-off of the first layer of timber lamellae after about 20 min of fire exposed additional fuel, leading to an increase in burning and increased temperatures and HRR; this process was repeated multiple times as deeper lamellae charred and fell off, exposing unburned timber each time. This cyclic behaviour is clearly evident in Fig. 2b. Experiment Beta 2 was manually extinguished shortly after a third cycle in HRR increase was observed.

Experiment Gamma, with three exposed surfaces, displayed HRR and compartment temperatures that remained elevated after experiencing an initial peak. The timber continued to burn and char (with some char fall-off occurring albeit with no discernible distinct influence on the burning regime) until the fire was manually extinguished after 80 min (Fig. 2c). The precise fire dynamics of these burning regimes is not the focus of the current paper; and in any case this has already been presented elsewhere [4,6]. The Alpha configuration is not included in the current analysis since it is more relevant to a discussion of auto-extinction and the thermal insult is not expected to vary greatly from other experiments where no auto-extinction occurred (e.g. Gamma1).

Fig. 3 shows the variation of in-depth temperatures in the ceiling CLT panel with time experiments Beta1, Beta2, and Gamma1. For each scenario, the mean temperatures across all thermocouple locations where the same in-depth temperature measurements were taken (refer to Fig. 1) are given, along with shaded areas showing one standard deviation from the mean of the readings at these locations.

The heated depth is shown for 60 °C, 100 °C, and 200 °C, as is the char depth assumed on the basis of a 300 °C isotherm which is typical in fire research on timber. A 60 °C isotherm has been included in these plots because irreversible changes in the timber's mechanical properties have been suggested to occur in this range [40]. A temperature of 100 °C has been used because of its significance for moisture loss, and because prior studies have shown that reductions in strength and stiffness of timber are most pronounced up to this point with less severe reductions of mechanical properties above 100 °C [41–44]. An isotherm for 200 °C is also shown because temperatures of 200 °C are often used to signify the onset of pyrolysis [45]. At 300 °C pyrolysis of the timber is assumed to be complete [18,42,46].

To determine the heated depths shown in Fig. 3, discrete temperature readings at various depths were used to fit a spline curve with a smoothing parameter of 0.1 (note that a smoothing parameter of zero fits a linear regression curve, whereas a smoothing parameter of unity fits a piecewise polynomial curve which passes through all data points precisely) at each time step. This was repeated for each location, each experiment, and each exposed timber surface. Variation of thermal penetration depths with time were then determined from the resulting curve fits based on the deepest distance from the fire exposed timber surface where the corresponding temperature was measured.

It is noteworthy that a trade-off exists in choosing a value for the smoothing parameter. A linear fit (i.e. smoothing parameter = 0) fails to capture steep temperature gradients and therefore leads to conservative results and an overestimation of loss of structural capacity. Conversely, a smoothing parameter close to unity will reduce the

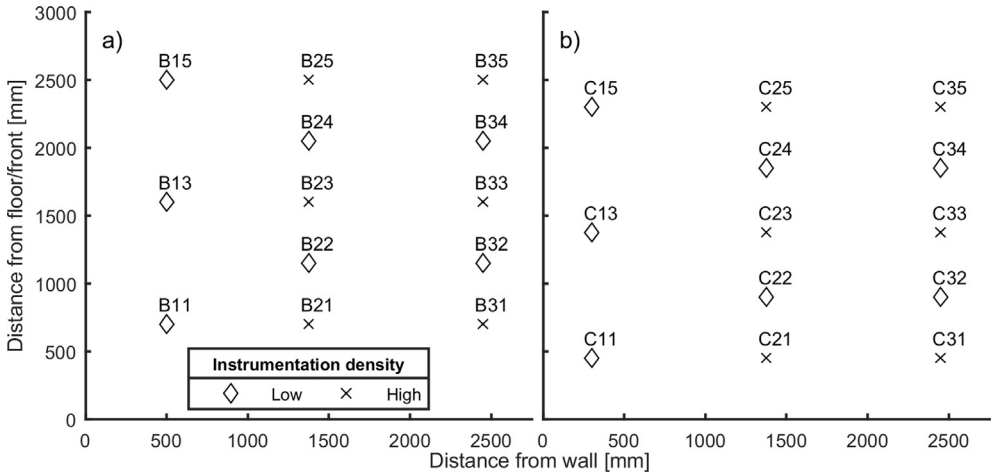

Fig. 1. Thermocouple positions across the (a) back wall and (b) ceiling for all experiments.

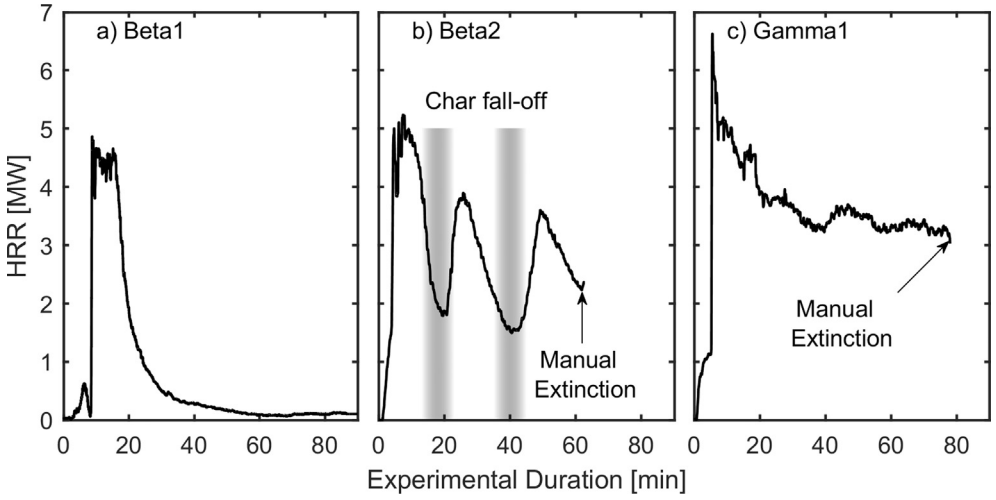

Fig. 2. CLT compartment heat release rates showing three distinct possible compartment fire dynamics phenomena: (a) auto extinction, (b) cyclic HRR, and (c) continued burning with eventual manual extinction.

interpolation performance between thermocouple depths and result in large scatter, thereby corrupting the fundamental purpose of the fitting exercise. The authors have arbitrarily selected a curve fitting parameter of 0.1, since it appears to give a reasonable balance between these competing constraints.

The spatial mean charring rate over all thermocouple positions in the ceiling panels for Beta1, Beta2, and Gamma1 experiments is shown in Fig. 4, again along with shaded areas showing one standard deviation

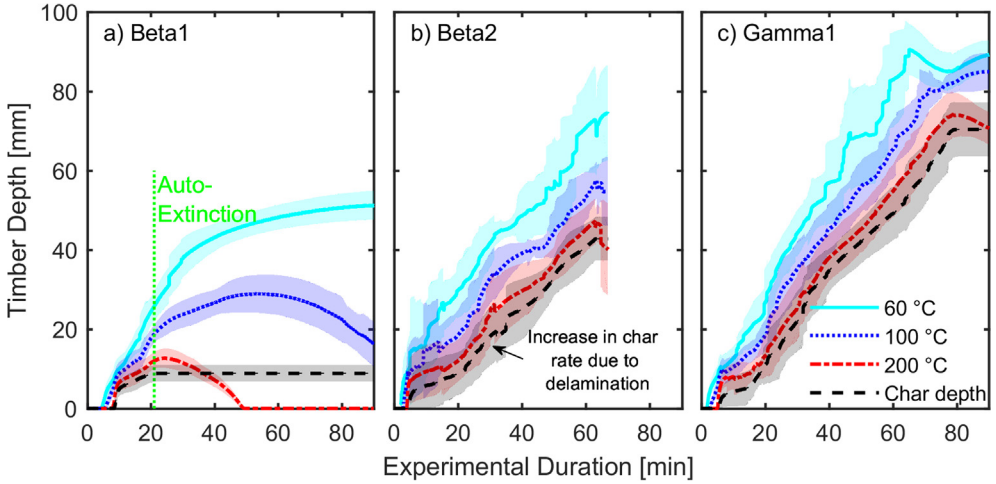

Fig. 3. Thermal penetration depths from the location of the original timber surface (selected isotherms, as noted in the text) in the ceilings of the experiments listed in Fig. 2. Shaded areas denote one standard deviation from the mean at each of the different measurement positions.

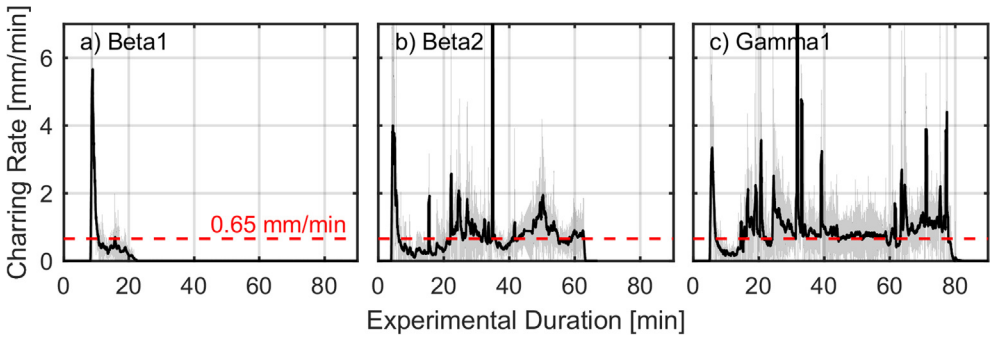

Fig. 4. Charring rates averaged over all positions, with one standard deviation shown as the shaded area, for the ceilings of experiments, Beta1, Beta2, and Gamma1, including constant charring rate of 0.65 mm/min shown for comparison.

from the mean at each position. An initial peak charring rate is observed early in all three experiments. This subsequently reduced due to the formation of a char layer with a quasi-steady depth, which insulated the underlying timber causing the pyrolysis front to gradually progress in depth. The base charring rate for solid timber, i.e. 0.65 mm/min, provided in the Eurocodes [17] is also shown in these plots. It should be noted that the charring rates presented here were not measured directly, but have been calculated from the location of the 300 °C isotherm using the method validated by Bartlett et al. [47] for cross-laminated timber panels. No final charring depths were measured, resulting in some uncertainty about the final depths. A detailed description of charring depths and rates across the walls and ceilings is a work in progress and will be dealt with in a separate publication.

Experiment Beta1 displays a charring rate that reduces to zero almost immediately after auto-extinction (see Fig. 3a). For the other two experiments shown, multiple peaks in the charring rate are observed as the burning duration progresses. These are likely caused by successive localised char fall-off, thereby exposing uncharred timber to the fire and temporarily increasing the local charring rate. This is considered to be the main driver for the cyclic increase and decrease in the HRR shown in Fig. 1b. A similar behaviour can be observed in plots of charring rates for the back walls (Fig. 6). For the wall in Experiment Beta 1 (Fig. 6a) a second peak in the charring rate is evident; this is most likely caused by local char fall-off, yet any additional fuel contribution from this appears not to have been sufficient to prevent subsequent auto-extinction in this case. Additional research is needed to better understand the various parameters potentially affecting auto-extinction so that structural fire engineering designers can make confident design assumptions regarding the prognosis that this will occur (or not) in real design scenarios. For all experiments presented here it is observed that, where no peaks in charring rate occur, the charring rates stabilise close to the base charring rate of 0.65 mm/min. This behaviour is already well documented and utilised for modern design approaches to the charring rate, which additionally recommend an increase in the base charring rate when char fall-off is expected to occur [48].

In Figs. 3 and 5 it is clear that the temperature development for Experiment Beta1, in which auto-extinction occurred, is fundamentally different from the other two cases presented. Auto-extinction occurs at around 20 min for Beta1, and subsequently the depth of the char layer (i.e. the 300 °C isotherm) remains constant indicating that charring has effectively stopped. All strength and stiffness in the char are assumed to be irrecoverably lost. Thus, despite the 300 °C isotherm retreating upon cooling, the formation of char is permanent and irreversible.

After charring stops, however, the thermal wave continues to progress deeper into the uncharred timber. For example, the depth of the 200 °C isotherm continues to increase for an additional 10 min in this case, before cooling dominates. The 100 °C isotherm, which is associated with considerable reductions in mechanical properties (e.g. 75% loss of strength and 65% loss of elastic modulus [17]) of the timber, continues to progress into the element for 30 min beyond burnout. For the 60 °C isotherm this progression continues until the experiment is terminated (i.e. the instrumentation is switched off and water is applied to arrest smouldering).

Experiments Beta2 and Gamma1 did not experience auto-extinction. This is reflected in the charring depth plots in Figs. 3 and 5, which show char depth increases up until the point of extinction in both cases. It is noteworthy that data for experiments Beta2 and Gamma1 are more erratic; this can be attributed to the occurrence of spatially non-uniform char fall-off that was observed directly during the experiments. This leads to sudden localised loss of the insulating char and therefore localised increases in charring rate and internal temperatures in these locations; this manifests in the data as increased variation about the mean values.

Comparing Fig. 3(a) and Fig. 5(a), the standard deviation between the measured locations varies between the ceiling and back wall measurements for Experiment Beta1. This is not observed for experiments Beta2 and Gamma1, where differences between measurement locations were influenced by the occurrence of char fall-off and the changing fire dynamics within the compartments as already noted. Also, owing to the increased burning durations of Beta2 and Gamma1 as compared with Beta1, these fires progressed to become ventilation controlled ‘Regime I’ fires [49], while Experiment Beta1 did not last long enough to establish a deep smoke layer, and the walls were therefore subjected to spatially varying heat fluxes (compared with the ceiling, which was exposed to a more uniform hot smoke layer) with height from the plume from the original fuel load, i.e. a ‘Regime II’ fire [49].

It is also noteworthy that in the final stages of Experiment Gamma1 the temperature readings in the back wall appear somewhat erratic. This is likely because forced extinction was applied to this wall through water spray, thus causing rapid cooling of the wall. This is not seen for the ceiling, which instead cooled due to reduced compartment temperatures.

Another observation from Figs. 3 and 5 is that the increase in char depth and thermal penetration in Experiment Beta2, thought to be caused at least partly by fall-off of char, occurs when the calculated char depth is less than 20 mm (the width of each of the individual lamellae). This suggests that char fall-off at glue lines may in some cases occur before the 300 °C isotherm penetrates to the glue line; this could possibly be due to softening/weakening of glue lines. Additional research is needed to better understand, quantify, and prevent char fall-off.

6. Load bearing capacity in fire

The current paper examines thermal penetration into the CLT panels and its potential (theoretical) consequences for their load bearing capacities in both bending and axial compression. From the observed temperatures in Figs. 3a and 5a it is clear that a thermal wave continues to propagate in-depth after burnout and auto-extinction. The areas heated between 200 °C and 300 °C reduce in the cases shown, whereas

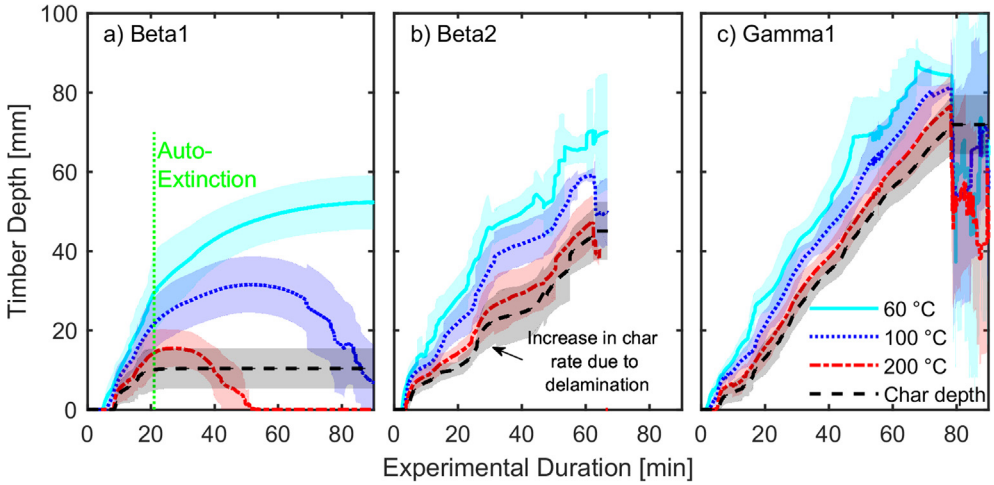

Fig. 5. Thermal penetration depths from the location of the original timber surface (selected isotherms, as noted in the text) in the back walls of the experiments listed in Fig. 2. Shaded areas denote one standard deviation of different measurement positions.

additional timber is heated to 100 °C. From a structural fire engineering perspective this is problematic, since the majority of loss of strength and stiffness for timber occurs up to 100 °C and is complete by 300 °C. According to the Structural Eurocodes [17], timber loses 75% and 65% of its compressive strength and stiffness parallel to the grain, respectively, at 100 °C when heated under standard fire conditions. Whilst these losses in mechanical properties have been derived for standard fire exposures they agree reasonably well with empirical studies on heated timber [43], and are therefore considered to be sufficiently applicable for the illustrative analyses presented in the current paper. Thus, the post burnout thermal wave phenomenon appears likely to be significant for timber elements.

The increase of temperatures in the decay phase after burnout is not typically considered in structural fire design for timber, and the specific consequences of this are currently unknown to the knowledge of the authors. This concern is particularly relevant for buildings with defend-in-place fire strategies and when accounting for fire service intervention considerations.

The following sections provide a quantification of the theoretical magnitudes of additional decay phase loss of load-bearing capacity in both flexural and compressive loading scenarios for CLT elements. The section ends with special consideration given to glulam columns supporting compressive loads.

6.1. Analysis of residual load bearing capacity

To assess the structural load bearing capacity of CLT elements based on the temperatures measured in the experiments presented above, the measured temperatures were fitted to smoothing functions to give approximate in-depth temperature gradients through the timber sections. These were then used, in conjunction with a computational cross-sectional analysis program, and the timber mechanical property reduction curves given in Eurocode 5 [17], to predict the remaining strength and stiffness of the timber with temperature and location over the cross-section, and hence the overall load bearing capacity in bending (in this section) or compression (in the following section).

The normal cross-sectional analysis assumptions that are widely used within structural engineering are deployed herein; it is assumed that plane sections remain plane for all loading conditions and that shear deformations between the timber lamellae can be ignored. This is based on the assumption that shear deformations in CLT become negligible for span to depth ratios of greater than 20 [51]. In addition, recent research has demonstrated that rolling shear failure is unlikely in fire exposed CLT members [52]. The current analysis is concerned with the theoretical relative strength loss throughout a real compartment fire, notably including a decay phase and the influence of the previously noted thermal wave.

Before the distribution of elastic modulus over a cross-section can be determined, the depth of the neutral axis must be assumed since the reduction of the elastic modulus of timber with increasing temperature varies depending on whether timber is in tension or compression [17]. The elastic modulus distribution is in turn needed to determine the neutral axis depth; hence, an iterative analysis approach is required. At each assumed curvature, an initial estimation of the neutral axis location is used to find the elastic modulus distribution over the cross-section. From this, the stress distribution is determined as the product of elastic modulus and strain in each elemental slice. The actual neutral axis depth is then found via Newton-Raphson iterations to ensure axial

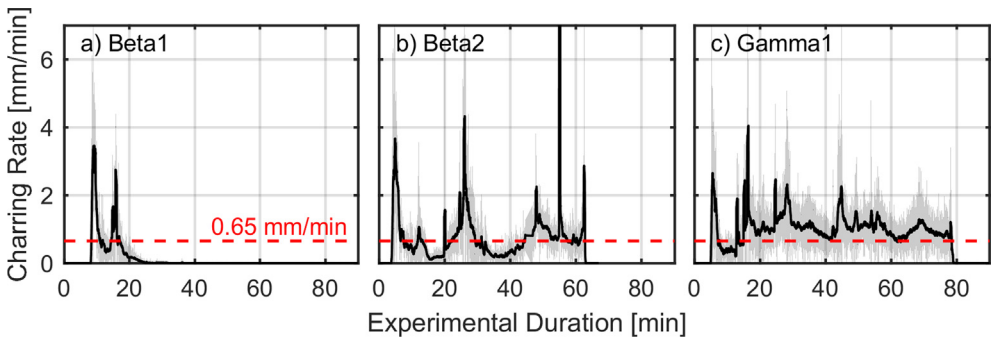

Fig. 6. Charring rates averaged over all positions, with one standard deviation shown as the shaded area, for the back walls of experiments, Beta1, Beta2, and Gamma1, including constant charring rate of 0.65 mm/min shown for comparison.

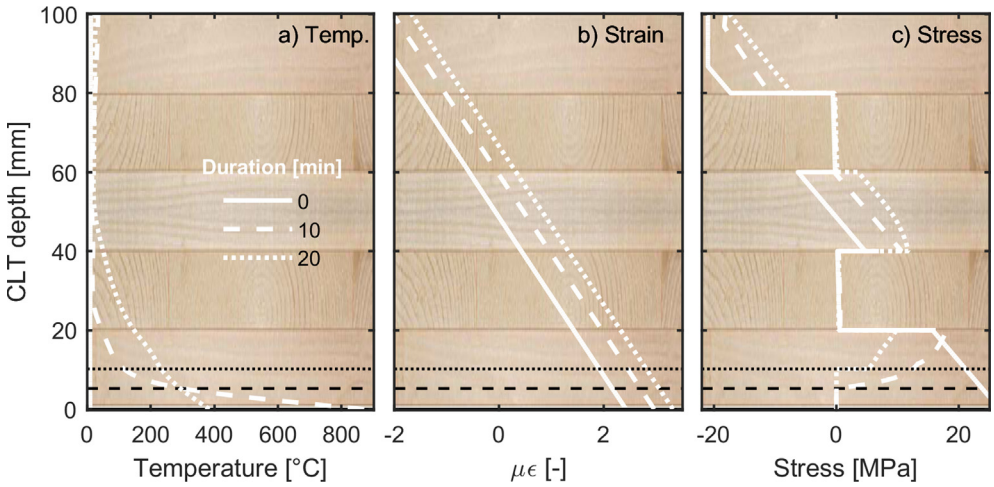

Fig. 7. Illustration of (a) temperature, (b) strain and (c) stress distribution through a CLT cross-section at different times during Experiment Beta1. Char depth is shown in black.

equilibrium over the cross-section, and this then updates the elastic modulus for each slice and thus the assumed stress distribution

In compression, the stress-strain behaviour of the timber is assumed to be elastic-perfectly plastic. Once the compressive yield strength, which also reduces with increasing temperature in assumed accordance with the Structural Eurocodes, is exceeded, yielding is assumed to occur and plasticity is applied to the affected elements, i.e. the stress is not increased beyond the assumed yield strength. In this way, the curvature is increased linearly until either the tensile strength or the ultimate strain in compression are exceeded in any elemental slice. Failure of the cross-section, and thus its ultimate flexural capacity, can then be computed from the stress distribution and the determined neutral axis depth. This is similar to a procedure suggested for analysis of timber at ambient conditions by Buchanan [53], with the additional consideration of thermally induced variations in strength and stiffness in accordance with the reduction curves suggested by Eurocode 5 [17].

The basic process for the above calculation procedure is shown schematically in Fig. 7, which shows the temperature distribution in the timber at various times during Experiment Beta1. Alongside the temperatures are the respective strain and stress distributions at failure.

The cross-section is divided into elemental slices (layers), allowing determination of the stress at failure in each layer from the distributions shown, for example, in Fig. 7c. In combination with the depth of the neutral axis, the moment capacity can then be calculated based on simple mechanics as in Eq. (1).

$$M_u = \sum_{1}^{n_e} \sigma_i A_i y_i \tag{1}$$

where σ is the stress, A is the area and y is the distance to the neutral axis of each element (layer) in the timber cross-section. The timber cross section was divided into 10,000 layers in the analyses presented herein since there were no significant restrictions on computational power while a significantly less refined grid could logically induce computational errors in areas of steep temperature gradients.

Timber is widely assumed to be elastic-brittle in tension and elastic-plastic in compression [54,55]. Tensile failure usually occurs where defects like knots or wanes exist in a cross-section. This has consequences for the design of timber members because the weakest point therefore governs bulk behaviour in tension. In bending, a smaller area is subjected to tensile stresses than in the case of pure tension, and thus the probability of randomly occurring defects causing a tensile failure reduces for elements in bending. The stress distribution must therefore be considered to assess the tensile failure strength in bending.

The calculations given herein are concerned with relative loss of structural capacity, and thus the reliance on choosing the correct material input parameters is minimal. Strength values at ambient temperature for the analyses were chosen in accordance with EN 338 [39] for a C24 timber strength class.

There is a paucity of available data on the yield and ultimate strain of heated timber in compression. Buchanan [56] proposes values between 0.004 and 0.05; a value of 0.05 was chosen for the simulations presented herein. This upper bound was chosen to assess the consequences of a ‘best case’ scenario, i.e. what is the worst that can happen under ‘good’ conditions.

6.2. Bending elements

The theoretical normalised bending capacity during the burning duration of the ceilings from the three aforementioned experiments is given in Fig. 8 for two possible scenarios: (1) a case where all losses of strength and stiffness of (uncharred) timber due to temperature are assumed to be fully recoverable, and (2) where strength and stiffness losses due to increased temperature are assumed to be fully irrecoverable, even for uncharred timber. The reality will lie somewhere between these two extremes. The authors are not aware of any available research that lends strong preference towards either of these assumptions at present.

The temperature data from the centre of the ceilings, where the highest bending moments can be expected to occur for simply-supported elements, have been used in the current analysis. Also displayed in Fig. 8 are alternative calculation results in which the experimental charring rate is used; however, instead of using the experimental heating data, a ZSL of 7 mm, as currently recommended in Eurocode 5 [17] for standard heating scenarios [12], is substituted to account for the reductions in strength of thermally affected timber beneath the char layer. The 7 mm ZSL was chosen over other available, and possibly improved, ZSL models simply for illustration and because the 7 mm value is currently codified in multiple national standards for the use of timber – and it has actually been used for the structural fire design of timber buildings.

From Fig. 8a, it is observed that reductions in ultimate bending capacity for the CLT slab after extinction are relatively minor in this case, if recovery of heated timber is assumed, and are unlikely to cause failure after burn out for the case of a severe but short fire that achieves auto-extinction. It is noteworthy that this fire has a burning duration of only about 21 min. If no strength and stiffness recovery is assumed, a continued loss of bending capacity can be observed after extinction for Experiment Beta1. This continued loss of capacity is proportional to the reductions that occur before extinction and is reasonably well captured

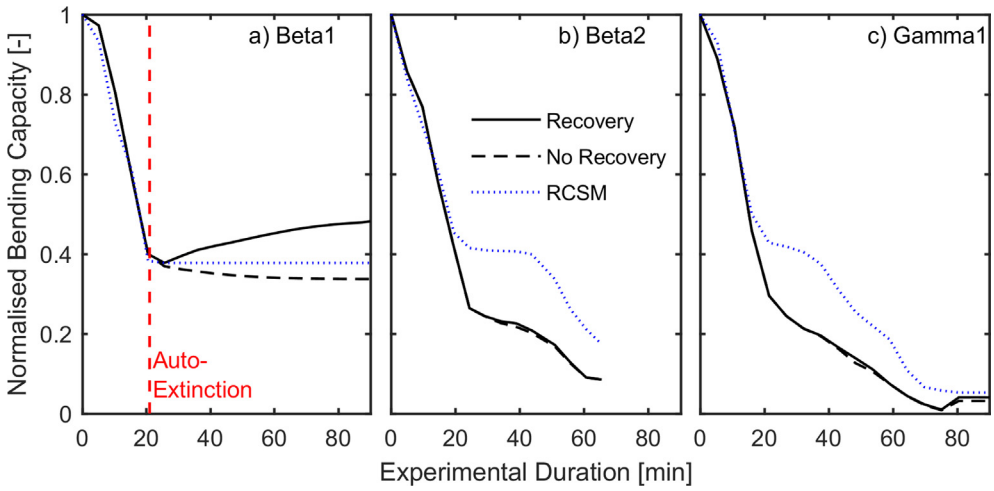

Fig. 8. Predicted reduction in bending capacity during full scale timber compartment experiments for (a) Beta1 – a short, severe fire with auto-extinction, (b) Beta2 – a longer fire with fluctuation of HRR due to char fall-off, and (c) Gamma1 – a fire with a semi constant ventilation controlled burning regime.

by the RCSM method.

The RCSM and the more advanced cross-sectional analysis method based agree well during the first 20 min of the fire; i.e. as the first lamella of the CLT chars under steep thermal gradients. This should be expected since the origin of the RCSM was developed and validated for glulam beams in bending during a standard fire [22] (which was developed based on the likely temperatures during flashover of a ventilation-controlled compartment fire). However, from Fig. 8b and c it can be seen that the RCSM estimates a slightly higher retention of bending capacity as the first crosswise layer is charred. This is particularly problematic because it is a reasonable assumption that CLT elements might be stressed to between 10%, for floors and ceilings, and 40%, for compression elements, of their ultimate capacity under the fire limit state loading. The ZSL only affects the crosswise layer, and any deeper thermal penetration is therefore not explicitly accounted for. Prior researchers have commented on this issue, and proposals for improved ZSL formulations specifically for CLT elements have been proposed elsewhere [48,57].

6.3. Compression elements

The failure of CLT bending elements in sagging is typically governed by tensile rupture of the most highly stressed timber lamella, and the compression face is unlikely to be significantly heated for simply supported planar CLT slabs. However, the reduction in strength and stiffness of timber is more severe in compression [17]. Because CLT walls are widely used to support gravity loads in multi-storey CLT buildings, it is important to investigate the theoretical crushing resistance of timber elements throughout a burnout fire scenario including the decay phase, particularly for fire-exposed CLT walls without encapsulation.

Compressive (crushing) strength is calculated by application of the ultimate compressive strain to the walls and calculation of the resulting stress distribution, both from the temperature gradients or based on the RCSM method (similar to the flexural case above). The results of this analysis are given in Fig. 9, where the concentric axial compressive strength and stiffness reductions in heated timber below the char layer are predicted to play significant roles in further reducing the relative load bearing capacities for more than one hour, from 73% to 62%, after auto-extinction occurs in Experiment Beta1.

It is physically impossible for a fixed depth ZSL to account for the continuous thermal wave after the charring halts. Here it must be noted that the ZSL method was never intended to be used in such situations, as it was derived based on simulations to determine capacity and failure in standard fire tests without a decay phase. To imply that a constant ZSL, whether 7 mm or any other fixed value, could account for the decay phase would be incorrect, and it is included here precisely to make this point. It is noteworthy that sudden increases in the relative crushing capacity in Fig. 9b–c are unrealistic and are an artefact of sudden discontinuities in the experimental thermocouple readings. This can occur within the empirical thermal profile data if, for example, a thermocouple becomes damaged and is removed from the analysis, or due to forced extinction by application of water.

6.4. Euler buckling capacity

At a height of 3 m the walls used in these experiments are relatively slender, and instability should therefore be considered in any assessment of their load bearing capacity. The theoretical Euler buckling capacities, for assumed ‘pinned-pinned’ support conditions, during the experiments were calculated by transforming the CLT into an effective cross-section based on the reduced elastic modulus from the temperature distributions and, similar to the calculations above, based on a ZSL in combination with the char depth that was calculated from experimental temperature measurements. It should be noted that the assumed pinned-pinned support conditions were chosen as a ’worst case’ scenario and that, in reality, some rotational stiffness is likely to be available from the connections, from continuity across multiple bays, and from three-dimensional effects.

The results of these calculations are shown in Fig. 10 for the three experiments discussed herein. For Experiment Beta1, the Euler buckling capacity closely matches until extinction occurs, after which the continued heating causes a further reduction in buckling resistance, albeit not as significant as the reduction for crushing shown in Fig. 9. For both experiments Beta2 and Gamma1, a reasonable agreement is observed throughout the burning periods aside from a short period in Experiment Beta2 resulting from the effect of the crosswise layer.

Compared to the pure crushing capacity shown in Fig. 9, the Euler capacity generally experiences a more severe reduction due to heating; this can be attributed to the increase in effective slenderness as the walls char and heat, which results in a second-order reduction in capacity and should, in the view of the authors, be explicitly accounted for during structural fire analysis of loadbearing timber in compression.

It is also noteworthy that the illustrative analysis presented herein assumes the initial (i.e. unloaded) elastic modulus of the cross sections. In reality, the presence of loading may further reduce the theoretical Euler capacity due to the plasticity of timber in compression. Additional research is urgently needed in this area so that rational design guidance can be suggested.

In reality, it would be unlikely for either pure crushing or pure Euler buckling to occur in a heated wall element, since the likely

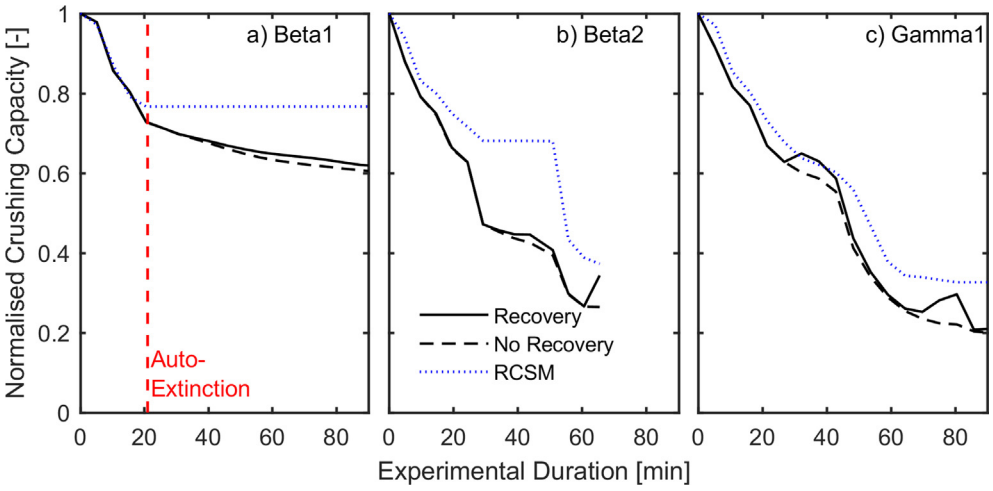

Fig. 9. Predicted reduction in pure compression (i.e. crushing) capacity of walls during full scale timber compartment experiments for (a) Beta1 – a short, severe fire with auto-extinction, (b) Beta2 – a longer fire with fluctuation of HRR due to char fall-off of timber lamellae, and (c) Gamma1 – a fire with a semi constant ventilation controlled burning regime.

asymmetrical heating of a CLT wall (i.e. with heating intended to be confined to a single fire compartment) would cause eccentricities in the loading and subject the cross-section to secondary bending moment effects, thereby increasing the propensity for buckling from secondary bending moments to occur in combination with plastic deformation in the extreme compression fibres.

The assessment of the resistance to instability for a semi-plastic cross-section would require knowledge of the deflection history of a particular element. Because the model utilised herein calculates ultimate limit states at a particular cross-section, and does not consider deflection histories, this is outside the scope in the current paper. This ought to be considered in practice however, and research into improved deflection-based failure models for CLT walls is currently underway.

6.5. Glulam columns

The observed temperature redistributions and the associated strength losses described herein are not limited to real fires, but have also been presented in the literature for timber elements heated in standard heating scenarios within fire testing furnaces [12]. Recently presented column fire resistance tests [35] subjected full-scale unloaded glulam columns, with side dimensions of 405 and 460 mm and a heights of 2100 mm, to 90 min of standard [12] fire exposure inside a fire testing furnace, before turning the furnace off and removing the furnace ceiling elements to allow for rapid cooling of the surrounding gas phase. The recorded temperatures were measured by plate thermometers inside the furnace and dropped from approximately 1000 °C to 300 °C in 33 min [35].

Full details of this experimental series (which was performed and reported by others) are not given here. However, in the context of the current discussion it is noteworthy that the reported temperature development through the depth of the columns can be used to analyse the theoretical loss of loadbearing capacity in a similar manner to the calculations for the crushing capacity of the CLT walls described above.

For glulam columns it was assumed that heating and charring are symmetrical on all sides. The resulting loss of crushing capacity, using calculations essentially identical to those described previously for CLT walls, however in this case with heating from all four sides, is shown in Fig. 11. It can be seen that the charring rate reduces slightly after the furnace is switched off – likely because the furnace floor and walls continue to radiate significantly even after the furnace burners are turned off and the ceiling removed – and eventually the char depth remains stationary. However, the predicted crushing capacity of the column continues to decrease, from 45% when the furnace is turned off down to 13% of its original value over a period of 2–3 h following the end of the heating phase. This is in part due to the continued charring, but more importantly due to continued heating from propagation of the thermal wave after the charring effectively stops.

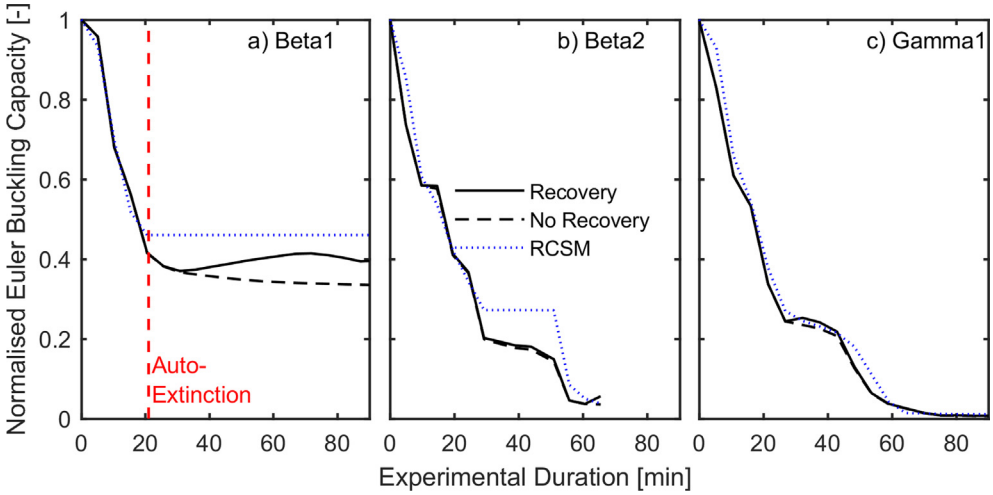

Fig. 10. Predicted reduction in Euler buckling capacity of walls during full scale timber compartment experiments for (a) Beta1 - a short, severe fire with auto-extinction, (b) Beta2 - a longer fire with fluctuation of HRR due to char fall-off, and (c) Gamma1 - a fire with a semi constant ventilation controlled burning regime.

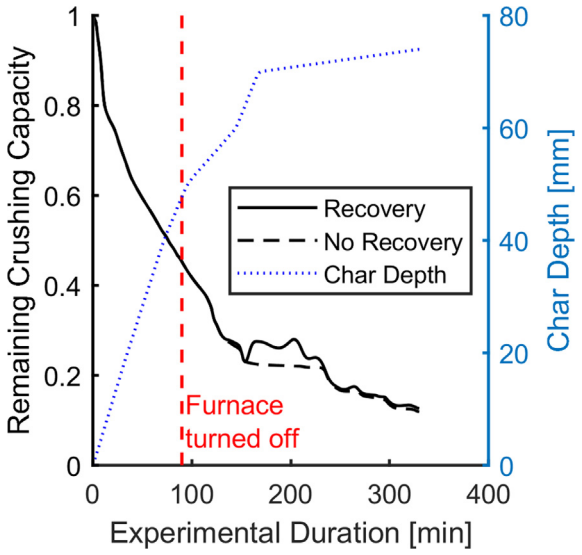

Fig. 11. Reduction in crushing capacity of a glulam column exposed on all sides to 90 min of standard furnace exposure and a subsequent manually imposed decay phase, based on data presented in [35].

7. Discussion and significance

From a structural fire engineering perspective, it is self-evident that collapse will eventually occur if no extinction occurs, as suggested by experiments Beta2 and Gamma1 discussed previously. Self-extinguishment is therefore considered critical for CLT buildings, for life safety in many cases and for property protection in all cases.

As already noted, the furnace testing was originally conceived as a comparative assessment method for structural elements exposed to real compartment fires, and was linked to real fire scenarios based on expected fuel loads and a fundamental desire that structures should maintain their loadbearing function until burnout of all movable fuel [58] (notably including internal linings and combustible finishes). In the compartment fire experiments described herein, the initial fuel load, consisting of wood cribs, was deliberately designed as the minimum required to generate post-flashover conditions, with an intentionally short period of pseudo-steady ventilation-controlled burning.

In a real fire, the burning duration may be longer, since higher compartment fuel loads can generally be expected in reality, and the thermal penetration depths could therefore be greater and have more severe consequences. This will depend on the amount of fuel in the compartment, but also on the type of fuel, the ventilation, and the fuel and compartment geometries. This also highlights the need to achieve auto-extinction in compartments where timber surfaces are exposed, or could reasonably be expected to become exposed, prior to burnout occurring.

Ambient design typically assumes a simplified stress distribution to consider the load bearing capacity of timber members in bending. Due to the temperature redistributions shown in Figs. 3 and 5, the stress distribution in timber during the decay phase of a fire can differ considerably from what is assumed by the simplified bending strength assumptions. The RCSM also simplifies design through a zero-strength layer and the subsequent treatment of the effective section as at ambient temperature. Under complex stress distributions to be expected in a decay phase such as that observed in Beta1, these two simplifications cannot be reconciled, and more rational design explicitly accounting for these effects should be undertaken.

The merit of the RCSM is its simplicity for use in predicting response under standard heating scenarios. It enables designers to quickly perform calculations to assess the standard fire resistance of timber members. However, with a recent increase of interest in CLT, the original concept for the ZSL has increasingly been challenged [25–27,57] within the research community.

The widespread application of the fire resistance concept as a framework for relative assessment of safety means that the accompanying verification methods, like the RCSM, have simple, binary outcomes in the form of either pass or fail of a fire resistance rating. This prevents engineers and researchers from confidently optimising laminated timber products during design with fire safety in mind.

The simplified analysis presented herein suggests that data are lacking as regards the structural assessment of mass timber elements under realistic heating (and post-heating decay) scenarios. Few data sets are available on strength and stiffness recovery of timber upon cooling. Knudson and Schniewind [60] suggested that timber heated to temperatures below 200 °C would increase in strength when reconditioned (i.e. when stored to reinstate a 12% moisture content). However, this same study also postulated that the elastic modulus is unaffected by heat; this contradicts all other studies in the field.

The recommended data (used herein) on the loss of mechanical properties upon heating are – strictly speaking – only valid for standard heating exposures [17], and all available data are derived from tests on individual timber boards rather than laminated timber systems. The actual mechanical response on heating for glulam or CLT could change if, for instance, the bond strength of the adhesives is affected. Additional research is also needed in this area.

A potential further consequence of deeper heated depths in the decay phase is weakening of the glue line and the possibility of debonding of char/lamella fall off occurring for engineered timber products. Debonding, other than char fall-off, occurs when the two adhering surfaces are timber and neither has charred completely. For standard fire resistance tests, the temperature gradient in the timber is assumed to be sufficiently steep so as to ensure that glue line temperatures are sufficiently low that debonding or loss of composite action can be avoided before charring of the affected timber occurs [61]. However, for prolonged heating with lower heat fluxes and shallow temperature gradients (e.g. during a decay phase) it has been shown from lap shear elevated temperature bond experiments that debonding may occur as a failure mode [62]; it has also been shown that local debonding can cause stress concentrations, and that these could develop into rolling shear failures [63]. A bond line temperature of 150 °C has been identified as critical by Craft for the weakening of PUR adhesives [64], however different formulations of adhesives can show considerable variation in thermal performance [65]. Additional research is also needed in this area.

8. Conclusions and recommendations

In depth temperatures of CLT elements in full-scale compartment fire experiments have been analysed and the theoretical reductions in load bearing capacity of exposed ceiling and wall elements predicted for illustrative purposes in this paper. It has been shown that the load bearing capacity of CLT walls and slabs can be expected to continue to reduce, to differing degrees, during the decay phase of a burnout fire. This occurs even after auto-extinction has been achieved and charring has ceased and is attributed to the continued propagation of a thermal wave beneath the char layer during the decay phase. This effect has also been shown to apply to glulam columns tested by others [35]. For simply-supported flexural elements heated from below the redistribution of temperatures does not appear to result in significant loss of capacity during the decay phase.

Comparisons have been provided for the theoretical load bearing capacity reductions between a cross sectional analysis model, which accounts for the actual temperature profiles in the timber and the resulting reduction in mechanical properties of the timber layers, versus a conventional RCSM model using a constant zero strength layer depth of 7 mm and the experimentally obtained charring rates. For slabs in

bending, it was found that the initial reduction in the ultimate moments agreed well between the two analysis approaches; this was, however, not the case once the weak cross-layers charred, as expected based on prior work by others [27].

The results presented in the current paper, and the accompanying theoretical considerations for the reduction in structural capacity, suggest that, for timber compartments with significant amounts of exposed timber structural elements, the fire dynamics and the thermal and structural response are closely interlinked and cannot be considered separately – as is explicitly done within the traditional structure fire resistance design framework that has been historically deployed for use with non-combustible structural systems (i.e. concrete and steel structures, or encapsulated timber). The conventional fire resistance framework, where structural safety in case of fire is provided essentially as a relative measure, cannot provide suitable means by which to optimise innovative laminated timber products, and also hinders the application of structural fire safety engineering as part of a holistic fire safety design approach in tall, engineered mass timber buildings.

8.1. Recommendations

A lack of data on the reduction in strength and elastic modulus for heated timber has been identified, especially since all existing data originated from solid timber boards and may not be fully applicable to laminated timber products including CLT and glulam. Research into the mechanical properties of heated, uncharred laminated timber is therefore urgently needed. Likewise, a lack of data on the residual strength of timber after being heated introduces uncertainty into the analyses of timber elements during the decay phase after auto-extinction.

Where buildings use exposed structural timber and rely on a defend-in-place fire strategy (as would be expected in mid- to high-rise residential timber buildings) designs should normally ensure auto-extinction will occur after the (moveable) fuel load has burnt out. The load bearing capacity of walls and columns will continue to deteriorate after burnout, and currently this is not explicitly accounted for in prescriptive fire resistance design (e.g. based on Table A2 in Approved Document B [66] or 4.1.3.1.2.1 in NFPA 5000 [67]).

Designers of timber buildings, and especially of tall timber buildings, should therefore consider the decay phase when specifying required member dimensions to maintain load bearing capacity during burnout fires. In order to carry out an engineering design of a mass timber building, close cooperation between the structural and fire engineering team will be necessary. Since the fire dynamics and the structural behaviour are interlinked and the heat transfer is more complex than for steel or concrete, the range of potential fires cannot be represented by a single temperature versus time exposure.

Acknowledgements

The authors gratefully acknowledge support from Arup and the University of Edinburgh to undertake the experiments from which this paper draws its primary data. The authors would also like to acknowledge support from the UK Engineering and Physical Sciences Research Council (EPSRC, EP/M508032/1), KLH, Rockwool International A/S, and SWG. The authors appreciate technical and physical support from Nikolai Gerasimov, Timothy Putzien and Mark Fenton. BRE, IFIC Forensics, and The Royal Academy of Engineering are acknowledged for their long-term support to Fire Safety Engineering research at the University of Edinburgh.

References

[1] The doomed city. The New York Times; 1871 10th October.
[2] Frost LE, Jones EL. The fire gap and the greater durability of nineteenth century cities. Plann Perspect 1989;4(3):333–47. https://doi.org/10.1080/02665438908725687.
[3] Buchanan AH. Fire resistance of multistorey timber buildings. In: Harada K, Matsuyama K, Himoto K, Nakamura Y, Wakatsuki K, editors. Fire science and technology 2015. Singapore: Springer; 2015. p. 9–16.
[4] Hadden RM, Bartlett AI, Hidalgo JP, Santamaria S, Wiesner F, Bisby LA, et al. Effects of exposed cross laminated timber on compartment fire dynamics. Fire Saf J 2017;91:480–9. https://doi.org/10.1016/j.firesaf.2017.03.074.
[5] Emberley R, Putynska CG, Bolanos A, Lucherini A, Solarte A, Soriguer D, et al. Description of small and large-scale cross laminated timber fire tests. Fire Saf J 2017;91:327–35. https://doi.org/10.1016/j.firesaf.2017.03.024.
[6] Bartlett AI, Hadden RM, Hidalgo JP, Santamaria S, Wiesner F, Bisby LA, et al. Auto-extinction of engineered timber: application to compartment fires with exposed timber surfaces. Fire Saf J 2017;91:407–13. https://doi.org/10.1016/j.firesaf.2017.03.050.
[7] Gorska C, Hidalgo JP, Torero JL. An experimental study of medium-scale compartment fire tests with exposed cross laminated timber. In: Nigro E, Bilotta A, editors. International fire safety symposium; June 7–9. Naples, Italy: Doppiavoce; 2017.
[8] Bartlett A, Hadden R, Bisby L, Lane B. Auto-extinction of engineered timber as a design methodology. In: Eberhardsteiner J, Winter W, Fadai A, Pöll M, editors. World Conference on Timber Engineering. Vienna; 2016.
[9] Emberley R, Do T, Yim J, Torero JL. Critical heat flux and mass loss rate for extinction of flaming combustion of timber. Fire Saf J 2017. https://doi.org/10.1016/j.firesaf.2017.03.008.
[10] The Building Regulations. In: England and Wales, editor. Westminster, UK: The Stationery Office Limited; 2010.
[11] EU Regulation. 305/2011 of the European Parliament and of the Council of 9 March 2011 laying down harmonised conditions for the marketing of construction products and repealing Council Directive 89/106. EEC2011.
[12] ISO. ISO 834-1-1999 Fire-resistance Test - Elements of Building Construction Part 1: General requirements. Geneva, Switzerland: International Organisation for Standardization; 2002.
[13] ASTM International. E119 Standard Test Methods for Fire Tests of Building Construction and Materials. West Conshohocken, Pennsylvania: ASTM International; 2016.
[14] CEN. EN 1363-1 Fire resistance tests Part 1: General Requirements. Brussels: European Committee for Standardisation; 2012.
[15] Thomas PH. The fire resistance required to survive a burn out. Fire Research Note 901; 1970.
[16] Law A, Hadden RM. Burnout means Burnout. SFPE Europe Mag 2017.;5.
[17] CEN. Eurocode 5. Design of timber structures. Part 1-2: General. Structural fire design. Brussels: European Committee for Standardisation; 2009.
[18] Frangi A, Fontana M, Knobloch M, Bochicchio G. Fire behaviour of cross-laminated solid timber panels. Fire Saf Sci 2008;9:1279–90.
[19] Schaffer EL. Structural Fire Design: Wood. DTIC Document, 1984.
[20] Gerhards CC. Effect of moisture content and temperature on the mechanical properties of wood: an analysis of immediate effects. Wood Fiber Sci 1982;14(1):4–36.
[21] Frangi A, Fontana M. Charring rates and temperature profiles of wood sections. Fire Mater 2003;27(2):91–102.
[22] Schaffer EL, Marx C, Bender D, Woeste F. Strength validation and fire endurance of glued-laminated timber beams. United States Department of Agriculture; 1986.
[23] Hopkin D, El-Rimawi J, Lennon T, Silberschmidt V. Effect of fire-induced damage on the uniaxial strength characteristics of solid timber: a numerical study. In: Journal of Physics: Conference Series: IOP Publishing; 2011. p. 012039.
[24] Schmid J, Just A, Klippel M, Fragiacomo M. The reduced cross-section method for evaluation of the fire resistance of timber members: discussion and determination of the zero-strength layer. Fire Technol 2015;51(6):1285–309. https://doi.org/10.1007/s10694-014-0421-6.
[25] Schmid J, Menis A, Fragiacomo M, Clemente I, Bochicchio G. Behaviour of loaded cross-laminated timber wall elements in fire conditions. Fire Technol 2015;51(6):1341–70. https://doi.org/10.1007/s10694-015-0516-8.
[26] Wiesner F, Randmael F, Wan W, Bisby L, Hadden RM. Structural response of cross-laminated timber compression elements exposed to fire. Fire Saf J 2017;91(Supplement C):56–67. https://doi.org/10.1016/j.firesaf.2017.05.010.
[27] Lineham SA, Thomson D, Bartlett AI, Bisby LA, Hadden RM. Structural response of fire-exposed cross-laminated timber beams under sustained loads. Fire Saf J 2016;85:23–34. https://doi.org/10.1016/j.firesaf.2016.08.002.
[28] Östman B, Mikkola E, Stein R, Frangi A, König J, Dhima D, et al. Fire safety in timber buildings - Technical guideline for Europe. Stockholm, Sweden: SP Technical Research Institute of Sweden; 2010.
[29] AWC. National design specification for wood construction. Washington, DC, USA: American Wood Council; 2016.
[30] AWC. Technical Report 10 - Calculating the Fire Resistance of Exposed Wood member. Washington, DC, USA: American Wood Council; 2016.
[31] Hopkin D, Schmid J, Friquin KL. Timber structures subject to non-standard fire exposure - advances & challenges. World Conference on Timber Engineering. Vienna, Austria; 2016.
[32] Katakura Y, Kinjo H, Hirashima T, Yusa S, Saito K. Deflection behaviour and load-bearing-period of structural glued laminated timber beams in fire including Colling phase. In: Moreya Garlock ME, Kodur VKR, editors. Structures in fire. Princeton: DEStech Publications, Inc.; 2016. p. 667–74.
[33] Hattori N, Ando K, Harada T, Kamikawa D, Miyabayashi M, Nishimura K, et al. Challenge to two-hours fire-resistive glued laminated timber made of Japanese cedar. In: Eberhardsteiner J, Winter W, Fadai A, Pöll M, editors. World Conference on Timber Engineering; August 22–25, 2016. Vienna, Austria: Vienna University of Technology; 2016.

[34] White RH, Woeste FE. Post-fire analysis of solid-sawn heavy timber beams; 2013.
[35] Andersen E. Fullstendig brannforløp i limtrekonstruksjoner. Oslo, Norway: Sweco, 2017 640670 Contract No.: RIBr01.
[36] Ellingwood B, Lin TD. Flexure and shear behavior of concrete beams during fires. J Struct Eng 1991;117(2):440–58. https://doi.org/10.1061/(ASCE)0733-9445(1991)117:2(440).
[37] Kodur V, Dwaikat M, Fike R. High-temperature properties of steel for fire resistance modeling of structures. J Mater Civ Eng 2010;22(5):423–34. https://doi.org/10.1061/(ASCE)MT.1943-5533.0000041.
[38] Hidalgo JP, Maluk C, Cowlard A, Abecassis-Empis C, Krajcovic M, Torero JL. A Thin Skin Calorimeter (TSC) for quantifying irradiation during large-scale fire testing. Int J Therm Sci 2017;112:383–94. https://doi.org/10.1016/j.ijthermalsci.2016.10.013.
[39] CEN. EN 338 Structural timber - Strength classes. Brussels: European Committee for Standardisation; 2009.
[40] White RH, Dietenberger M. Wood products: thermal degradation and fire; 2001.
[41] Van Zeeland I, Salinas J, Mehaffey J. Compressive strength of lumber at high temperatures. Fire Mater 2005;29(2):71–90.
[42] König J, Walleij L. Timber frame assemblies exposed to standard and parametric fires: part 2: a design model for standard fire exposure. Institutet för Träteknisk Forskning 2000;0001001:1–76.
[43] Young SA, Clancy P. Compression mechanical properties of wood at temperatures simulating fire conditions. Fire Mater 2001;25(3):83–93. https://doi.org/10.1002/fam.759.
[44] Jong F, Clancy P. Compression properties of wood as functions of moisture, stress and temperature. Fire Mater 2004;28(2–4):209–25.
[45] Browne FL. Theories of the combustion of wood and its control. Madison, Wis, USA: US Dept. of Agriculture, Forest Service, Forest Products Laboratory; 1958.
[46] Jönsson R, Timber Pettersson O. structures and fire: a review of the existing state of knowledge and research requirements: Swedish Council for. Build Res 1985.
[47] Bartlett A, Hadden R, Bisby L, Law A. Analysis of cross-laminated timber charring rates upon exposure to non-standard heating condition. In: 14th International Conference on Fire and Materials: Intersciences Communications; 2015. p. 667–81.
[48] Klippel M, Schmid J. Design of cross-laminated timber in fire. Struct Eng Int 2017;27(2):224–30.
[49] Hidalgo JP, Cowlard A, Abecassis-Empis C, Maluk C, Majdalani AH, Kahrmann S, et al. An experimental study of full-scale open floor plan enclosure fires. Fire Saf J 2017;89:22–40. https://doi.org/10.1016/j.firesaf.2017.02.002.
[51] Blass HJ, Fellmoser P. Design of solid wood panels with cross layers. In: 8th World Conference on Timber Engineering; 2004. p. 2004.
[52] Wiesner F, Bell D, Chaumont L, Bisby L, Deeny S. Rolling shear capacity of CLT at elevated temperature. World Conference on Timber Engineering. Seoul, South Korea; 2018.
[53] Buchanan AH. Combined bending and axial loading in lumber. J Struct Eng 1986;112(12):2592–609.
[54] Dinwoodie JM. Timber, its nature and behaviour. 2nd ed. New York, USA: Taylor & Francis; 2000.
[55] Bodig J, Jayne BA. Mechanics of wood and wood composites. New York, USA: Van Nostrand Reinhold Company Inc.; 1982.
[56] Strength Buchanan AH. model and design methods for bending and axial load interaction in timber members [Doctoral]. University of British Columbia; 1984.
[57] Schmid J, Klippel M, Just A, Frangi A. Review and analysis of fire resistance tests of timber members in bending, tension and compression with respect to the reduced cross-section method. Fire Saf J 2014;68:81–99.
[58] Ingberg SH. Tests of the severity of building fires. NFPA Quart 1928;22(1):43–61.
[60] Knudson RM, Schniewind AP. Performance of structural wood members exposed to fire. Forest Products J (USA) 1975.
[61] Klippel M, Frangi A. Einfluss des Klebstoffes auf das Brandverhalten von Brettschichtholz. Bauphysik 2012;34(4):142–52.
[62] Nicolaidis A, Emberley R, Fernando D, Torero JL. Thermally driven failure mode changes in bonded timber. In: Eberhardsteiner J, Winter W, Fadai A, Pöll M, editors. World conference on timber engineering. Vienna, Austria: Vienna University of Technology; 2016. p. Poster.
[63] Emberley R, Nicolaidis A, Fernando D, Torero JL. Changing failure modes of cross-laminated timber. In: Moreya Garlock ME, Kodur VKR, editors. Structures in fire. Princeton: DEStech Publications, Inc.; 2016. p. 643–9.
[64] Craft S. Fire performance of cross-laminated timber assemblies. In: Gagnon S, Pirvu C, editors. CLT handbook: cross-laminated timber. Québec: FPInnovations; 2011.
[65] Frangi A, Fontana M, Mischler A. Shear behaviour of bond lines in glued laminated timber beams at high temperatures. Wood Sci Technol 2004;38(2):119–26.
[66] The Building Regulations. Approved Document B (Fire Safety). London: NBS; 2013.
[67] Fire National. Protection Association. NFPA 5000: Building construction and safety code. NFPA 2018.